Iranian Journal of Physics Research, Vol. 24, No. 3, 2024
DOI: 10.47176/ijpr.24.3.71931

Ionoluminescence investigation of ambient humidity effects on CsI:Na scintillator crystal

T Nikbakht[*1] and H Faripour[2]

1. Physics & Accelerators Research School, Nuclear Science and Technology Research Institute (NSTRI), 14395-836, Tehran, Iran
2. Photonics and Quantum Technology Research School, Nuclear Science and Technology Research Institute (NSTRI), 14395-836, Tehran, Iran

E-mail: tnikbakht@aeoi.org.ir

(Received 07 July 2024 ; in final form 25 November 2024)

Abstract

Effects of ambient humidity on the ionoluminescence spectra of synthesized CsI:Na crystals were investigated for a time period of more than 500 days. Regarding the typical penetration depth of the applied ion beams in the ionoluminescence technique, it is suitable for investigating the humidity effects which are detectable at the outer surface of the scintillators. Three luminescence bands were observed for the samples, including CsI intrinsic luminescence and Na related bands, at ~ 310, 420 and 487 nm. It is shown that the relative intensity of the Na-related band, located at ~ 420 nm, significantly decreases over exposition time to humidity and exhibits considerable redshift. Since this band is the dominant one for detection purposes, its alteration leads to a decrease in the efficiency of CsI:Na scintillator. It was also observed that the relative intensity of this band for the sample which was grown in presence of trivial amount of humidity in the crucible, was initially much weaker and reacted less to the ambient humidity. The results of the present work demonstrate the capabilities of ionoluminescence as a suitable technique for scintillators' characterization.

Keywords: CsI:Na scintillator, ionoluminescence, humidity effect.

1. Introduction

CsI:Na is one of the most practical alkali halide scintillators, which regarding its physical properties, such as relatively high density, high scintillation light yield, good plasticity, excellent irradiation resistance [1-3], can be used in different cases including high energy physics, nuclear physics, nuclear radiation detection, detection of dark matter, nuclear medical imaging, space exploration, etc. [4]. It is also a suitable scintillator for pulse shape discrimination applications [5-7]. CsI:Na scintillator can easily be grown and therefore is cost effective, which suggests its utilization in different fields of applications. However, CsI:Na is almost a hygroscopic scintillator and will deteriorate in exposition to humidity. Therefore, studying the crystal behavior in such conditions can provide valuable information regarding the changes in its structure and scintillation properties. In 2014, effects of different humidity conditions on scintillation performance of CsI:Na crystals were reported by P. Yang and his coworkers [8]. They suggested that after exposing CsI:Na scintillator to water molecules, the Na ions diffuse out of the crystal and accumulate on its surface. Therefore, an "inactive" layer of polycrystalline appearance, which is almost depleted from Na ions, forms beneath the outer surface of the crystal. This phenomenon results in less intense Na related band in the spectra and, therefore, scintillation degradation of the crystals.

Ionoluminescence (IL) is a fast, highly sensitive and non-destructive technique which has been employed in several ion beam analysis laboratories for more than two decades [9-12]. It can explore different depths of the samples by changing the type and energy of the applied ion beam. Due to the high energy deposition density of the ion beam in materials, IL can provide different information compared to the cathodoluminescence (CL) or photoluminescence (PL) techniques. It can reveal new luminescence bands or result in shifts in the peak positions of the bands, which are indicative of the sample's characteristics. Therefore, it is considered as a suitable technique for investigating the luminescent samples [13-15].

Regarding the high capabilities of IL for successful investigation of different properties of organic and inorganic scintillators, such as their radiation hardness, radiation damage mechanisms and temperature response [16-23], it has been applied for studying the current

CsI:Na samples.

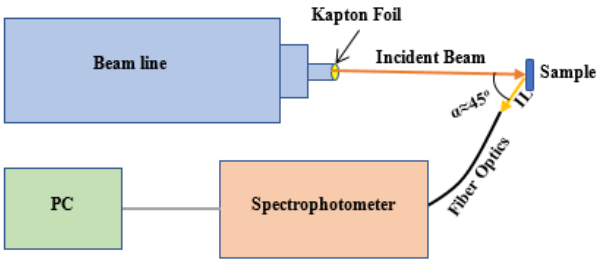

Figure 1. A schematic view of the in-air IL spectroscopy setup employed for running the experiments.

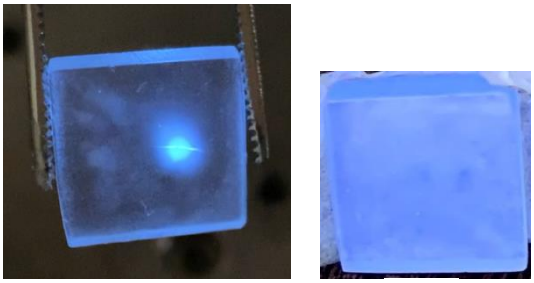

(a) **(b)**

Figure 2. (a) The IL of one of the samples irradiated with 2 MeV proton beam. (b) The opaqueness of the sample and small cracks on its surface after almost 2 years from its production is observable. Irradiation of the whole sample by the UV device.

In this research work, effects of ambient humidity on CsI:Na crystals is investigated by means of IL spectroscopy technique. Regarding the penetration depth of the typical ion beams which are employed in the IL technique, which is on the order of 10 μm, it reveals the surface alterations which occur due to ambient humidity on the outer surface of the scintillators. Whereas other luminescence inducers, such as X-ray, γ-ray or UV beams, explore incomparably greater depths of scintillators and are not able to clearly distinguish the effects of humidity on the samples. To the best of our knowledge, such kind of research is performed for the first time, in which the variation of the IL spectra of CsI:Na crystals, which are kept in mylar coverage, is investigated for a long time. It led to interesting results about the effects of ambient humidity on the crystals and also the nature of the luminescence bands of the scintillator.

2. Materials and methods

The high purity raw materials of the Merck company with 150 ppm sodium were used for producing CsI:Na crystals. The materials were heated up to 350° C and then dried for 10 hours under vacuum condition. The crystals were grown through Czochralski technique with a rate of 1 mm/hour. During the growth process of one crystal, there has been undesirable low amount of humidity in the crucible, which regarding the interaction of the material with water molecules, affected its characteristics (sample CSI2). For the case of the second crystal, the humidity was removed from the crucible to improve its properties (sample CSI1). More detailed information about the crystal growth process can be found in Ref. [24]. Two relatively thin sections of the CsI:Na crystals, with dimensions of ~ 2×2×0.4 cm^3, were selected to be studied in the present work.

The IL spectroscopy of the CsI:Na samples was performed in an in-air setup (figure 1), which generally results in high efficiency light collection. The in-air setup of IL, which has been employed only in few ion beam analysis laboratories in the world [10,11,25-28], is particularly suitable for weakly luminescent samples and allows direct collection of the spectra without limitations caused by additional optical devices, such as lenses, and vacuum chambers. An AvaSpec-ULS2048L spectrophotometer with 1.4 nm resolution in the wavelength range of 200-1100 nm was used to collect the spectra. The IL photons were transferred to the spectrophotometer through an optical fiber of 400 μm diameter, which was positioned ~ 5 mm from the sample surface (figure 1). The beam diameter on each sample was almost 1 mm (figure 2(a)). Proton beam of 2 MeV with a current of ~ 4 nA was employed for running the experiments. The IL spectra were collected within short integration time of 1 second. The fast Fourier transformation (FFT) technique is employed to remove the high frequency parts of the spectrum, which include the thermal noise and the air luminescence. The peaks' positions were also determined by the FFT which was performed by Origin (OriginLab, Northampton, MA). The experiments were repeated in distinct time intervals (196, 266 and 530 days after the first experiment) in the same experimental conditions to check the effect of the samples' hygroscopicity on their luminescence bands. In order to distinguish effects of proton ions and their penetration depth on the IL spectra, the experiments were also repeated (295 days after the first experiment) using helium ions of 2.4 MeV energy in the same experimental conditions. The integration time of the IL spectra produced by helium beam was 10 seconds. According to SRIM [29] calculations, 2 MeV proton ions after passing the ~7 μm Kapton foil as the extracting window of the beam line, and also 5 mm air column between the beam line and sample surface, lose their energy and degrade down to ~ 1.80 MeV protons, while 2.4 MeV helium ions after passing the same Kapton foil and 1 mm air column, degrade to ~ 400 keV helium ions. The penetration depths of 1.8 MeV proton beam and 400 keV helium beam in CsI are 123 μm and 5 μm, respectively. Therefore, the applied helium ions are able to explore the outer surface of each sample which is affected more by the ambient humidity [8]. Finally, in order to distinguish the effect of surface structure changes due to humidity, the UV-induced luminescence spectra of the samples were collected 1176 days after the first experiments, using a UVSL-25 device emitting a sharp line at the wavelength of 254 nm. The luminescence spectra were collected within 2 seconds. Regarding the penetration depth of the applied UV light and the transparency of the samples and their dimensions, in this experiment the luminescence originating from the whole bulk of the samples (figure 2(b)) will contribute in the spectra. This will allow to

distinguish between the surface luminescence and that of the bulk.

3. Results and discussion

The IL spectra of two different points, denoted as Data1 and Data2, on each CsI:Na sample (CSI1 and CSI2) collected in the in-air setup are presented in figure 3 (a,b). All the spectra exhibit three relatively broad bands with almost the same peak positions. The band peaking at 308-311 nm in the spectra is known as the intrinsic luminescence of the undoped CsI scintillator. It originates from self-trapped excitons and is known as a fast (~ 10 ns) emission band. The second band peaking at 415-420 nm with a decay time of 630 ns, is attributed to Na ions in CsI:Na crystal [30]. Regarding the sensitive wavelength range of PMTs, this is the band which plays the most important role in detection purposes. Therefore, the main focus of this work will be on its behavior. It seems that the existence of the third band peaking at 484-487 nm, has not been reported as a common luminescence band for CsI:Na scintillator. However, J.Ch. Hsu et al. [30], reported a shoulder appearing at ~ 470 nm in the X-ray luminescence spectra of CsI:Na and ascribed it to Na dopant.

Comparing the spectra of the two samples (in figure 3), it can be seen that in sample CSI2, the bands at 415-417 and 486-487 are considerably weaker than the corresponding intrinsic luminescence band at 308 nm, while in sample CSI1, the intrinsic luminescence bands at 310-311 nm are considerably weaker than the corresponding bands in longer wavelengths of the spectra. It seems that for the case of sample CSI2, during the crystal formation water molecules compete with Na atoms for occupying the network positions in the crystal. Therefore, the reason behind weaker intensities of the Na-related band in sample CSI2 is likely due to lower concentration of Na atoms in its crystalline lattice.

In order to investigate the CsI:Na behavior after being exposed to ambient humidity, the experiments were repeated some months later (196, 266 and 530 days after the first experiment), during which the transparency of the samples had reduced gradually (figure 2(a)) while they had been conserved in a Mylar coverage. The resulting IL spectra of the samples are presented in figures 4, 5 and 6. Humidity can both affect the optical properties of the scintillation crystals and the luminescence centers in them. Comparing the spectra in figures 4-6 with those in figure 3, it can be seen that over time the second luminescence band in the spectra undergoes considerable redshift, while the positions of the other bands remain almost unchanged. Moreover, the intensity of this band has reduced in relation to that of the third corresponding band, and also its shape has slightly deformed. This phenomenon explains the detection efficiency reduction of the scintillator.

In order to compare the effect of the probed depth of the samples on their IL spectra, 295 days after the first experiments, 2.4 MeV helium beam was used in the same experimental setup to provide the IL spectra which are presented in figure 7. Given the penetration depth of the helium ions, which is approximately 4% of that of the proton beam, humidity is expected to significantly affect the second peak in the spectra, as the effect of humidity is much greater on the outer layers of the samples. From figure 7, it can be seen that the resulting spectra are similar to those obtained by the proton beam, except that the second luminescence band appeared as a shoulder instead of a separate peak. Such observations confirm the effects of humidity on the surface structure of the scintillator.

Finally, the luminescence spectra of the samples, induced by 254 nm UV light, were collected and presented in figure 8. The sharp lines in the spectra are ascribed to the UV device, as it is shown in the inset (figure 8(b)). As expected, the first peak which is attributed to the undoped CSI crystal is absent in the spectra. Due to the transparency of the samples, the UV light that irradiates all over their area, entirely penetrates in them (figure 2(b)). Therefore, the second peak in the spectrum of sample CSI1 is less affected compared to the initial spectrum (figure 3(a)), since the deeper area of the sample is less affected by the ambient humidity. However, the second peak in the spectrum of sample CSI2 is considerably different from that of the initial one (figure 3(b)), which could be due to its production process and the fact that the whole volume of this sample had already been affected by the humidity. It should be noted that in comparison to the helium ion spectra (figure 7), the second bands in the UV spectra (figure 8) are presented as completely separate ones, which is due to the different penetration depths of the applied helium ions and the UV light. Moreover, given the relatively weaker intensities of the second peaks in the spectra of figure 8, in comparison to figure 3, it can be inferred that absorption of humidity results in lowering the efficiency of the bulk scintillator.

4. Conclusion

The IL technique was applied to investigate the ambient humidity effect on CsI:Na crystal scintillators. For this purpose, variations of the IL spectra of the samples, which have been kept in mylar coverage, were investigated for more than one year. It led to interesting results about the effects of humidity on the luminescence behavior of the samples which are mostly observable at their outer surfaces. Variation in the relative intensities of the Na-related peak in the IL spectra, initially located at ~ 420 nm, including its deformation and redshift, have been observed in the experiments. Application of helium ion beam and UV light, with respectively shallow and deep penetration depths in the samples, also confirm the effects of ambient humidity on the outer surface of the scintillator which result in lower efficiency of the scintillator. The results of the current work suggest application of IL, as a highly-sensitive technique, for scintillators' characterization. More subsequent researches are required to reveal detailed information about the effects of humidity on the CsI:Na scintillator.

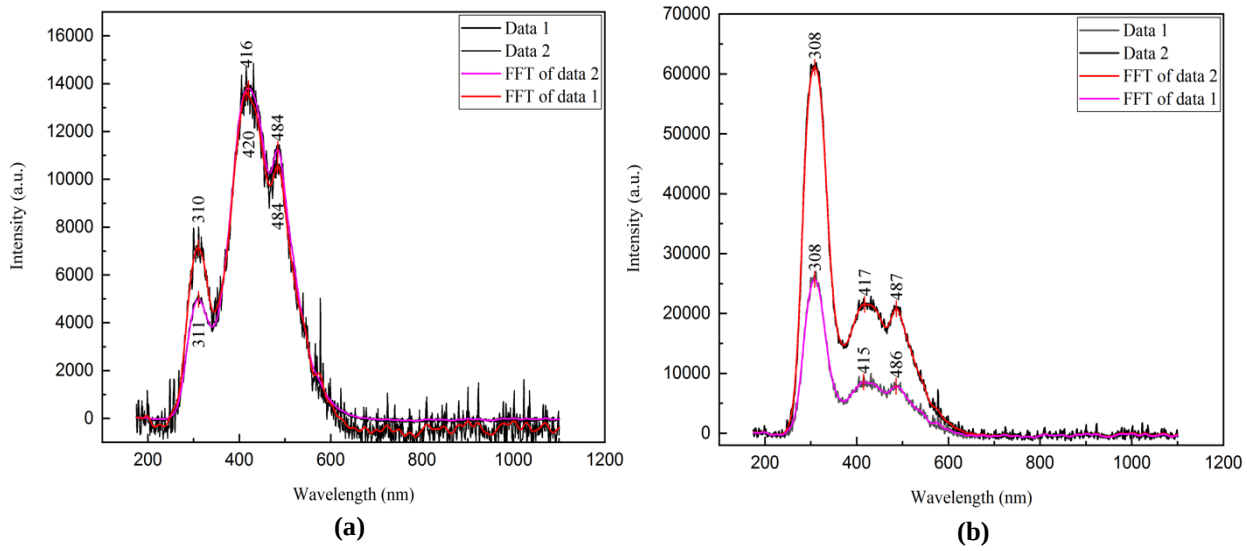

Figure 3. The initial IL spectra of two separate points, denoted as Data1 and Data2, on samples CSI1 (a) and CSI2 (b). Attempts to remove thermal noise of the spectra by means of FFT filter is shown via red and pink curves.

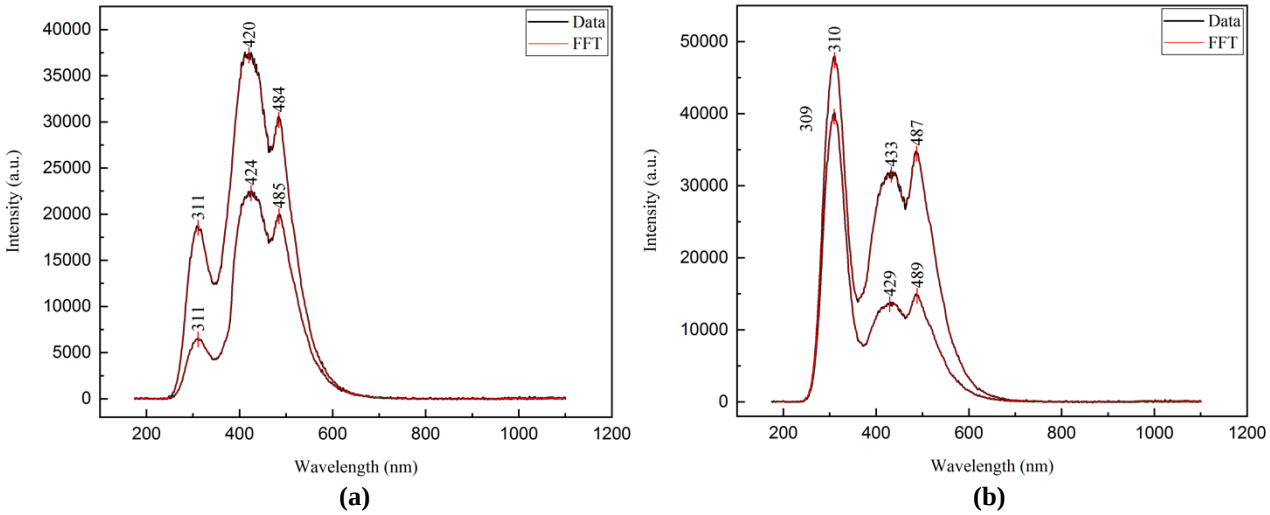

Figure 4. The IL spectra of two separate points on samples CSI1 (a) and CSI2 (b), collected 196 days after the initial experiments. Attempts to remove thermal noise of the spectra by means of FFT filter is shown via red curves.

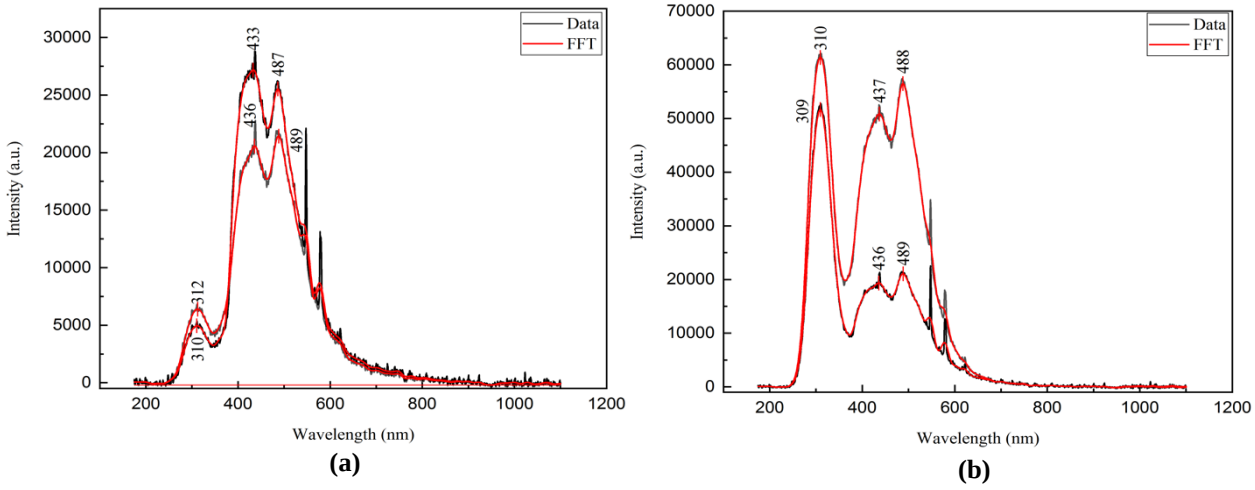

Figure 5. The IL spectra of two separate points on samples CSI1 (a) and CSI2 (b), collected 266 days after the initial experiments. Attempts to remove thermal noise of the spectra by means of FFT filter is shown via red curves.

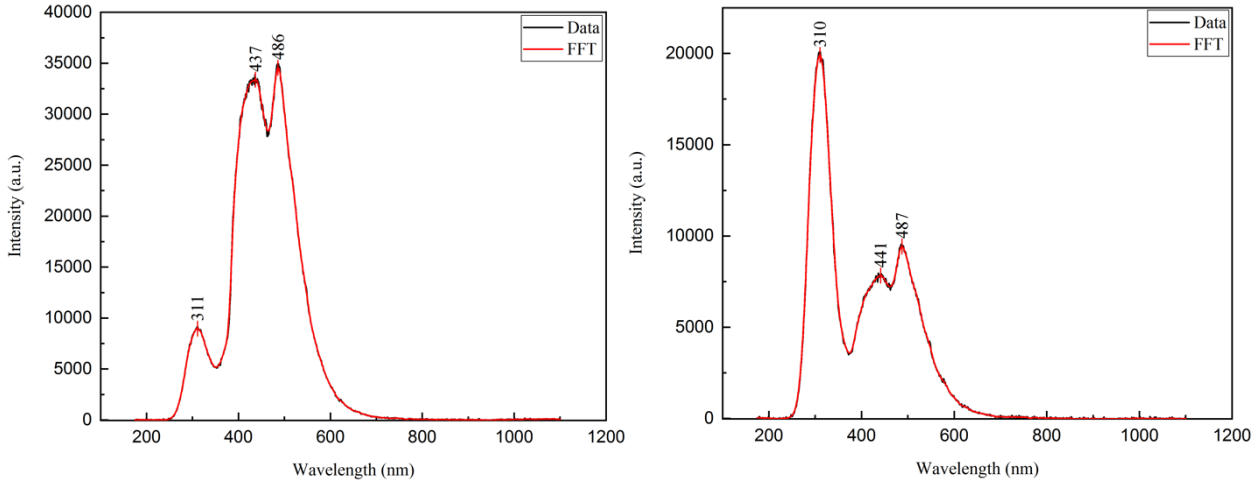

Figure 6. The IL spectra of samples CSI1 (a) and CSI2 (b), collected 530 days after the initial experiments. Attempts to remove thermal noise of the spectra by means of FFT filter is shown via red curves.

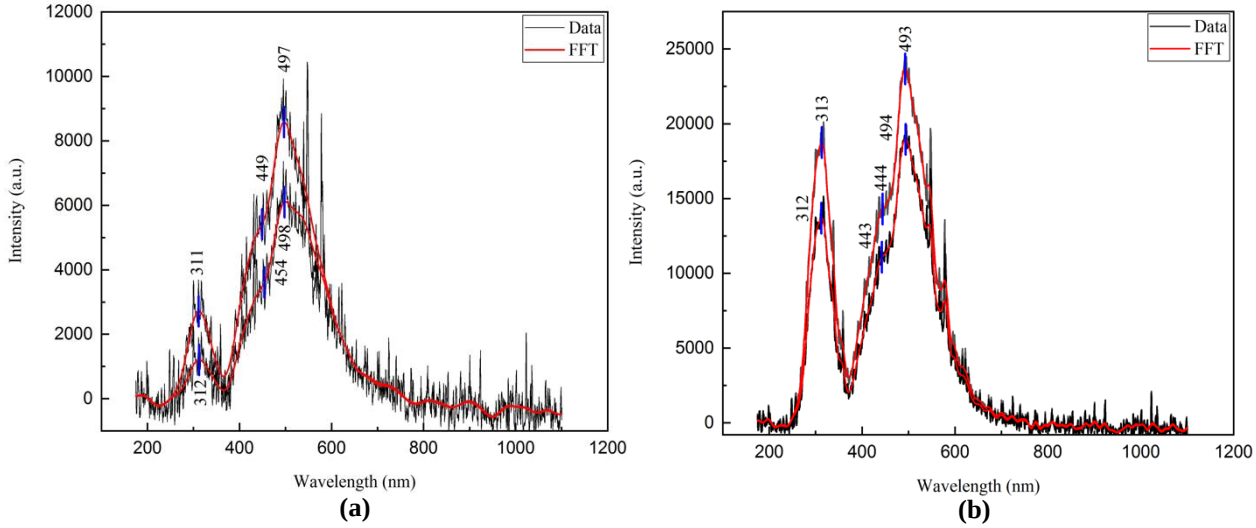

Figure 7. The IL spectra of two separate points on samples CSI1 (a) and CSI2 (b), collected 295 days after the initial experiments, using 2.4 MeV helium ions. Attempts to remove thermal noise of the spectra by means of FFT filter is shown via red curves.

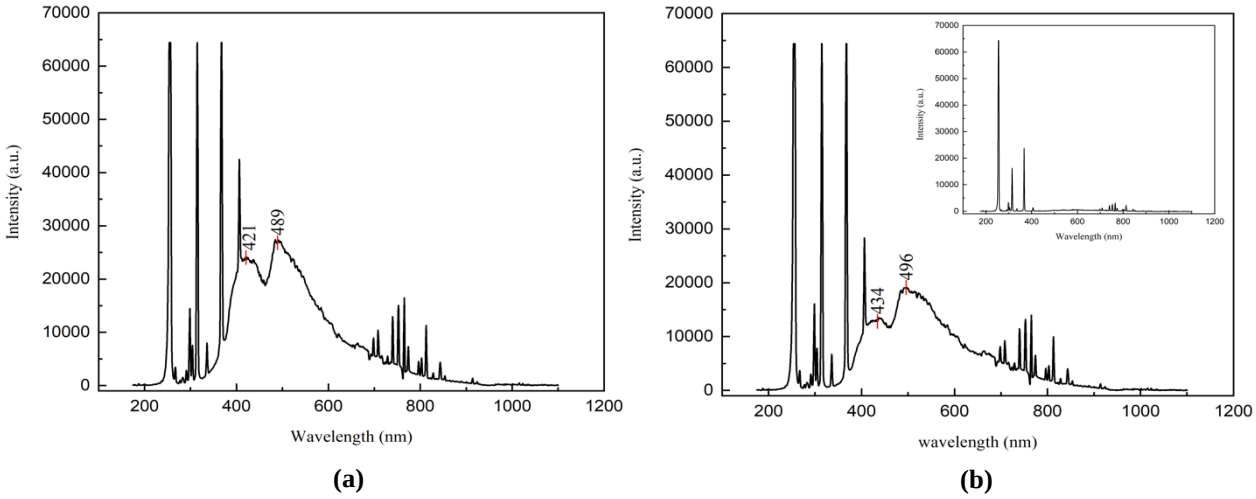

Figure 8. The 254 nm UV-induced luminescence spectra of the samples CSI1 (a) and CSI2 (b), collected for the integration time of 2 s, 1176 days after the initial experiments. The sharp lines in the spectra are ascribed to the UV device, which the most intense ones are saturated. The spectrum of the UV device is presented in the inset (b).

References

1. K Imanaka, A H Kayal, A Mezger, and J Rossel, *Phys. Status Solidi B* **108** (1981) 449.
2. V Yakovlev, L Trefilova, A Meleshko, and Y Ganja, *J. Lumin*. **131** (2011) 2579.
3. E Khodadoost, and M A Araghi, *Nucl. Instrum. Methods Phys. Res. A*, **942** (2019) 162351.
4. X Ouyang, B Liu, X Xiang, L Chen, M Xu, X Song, J Ruan, J Liu, Ch Chen, Zh Zhu, and Y Li, *Nucl. Instrum. Methods Phys. Res. A*, **969** (2020) 164007.
5. X Sun, J Lu, T Hu, L Zhou, J Cao, Y Wang, L Zhan, B Yu, X Cai, J Fang, Y Xie, Zh An, Zh Wang, Zh Xue, A Zhang, Q Lu, F Ning, Y Ge, and Y Liu, *Nucl. Instrum. Methods Phys. Res. A*, **642** (2011) 52.
6. H Yuan, F Liy, H Zheng, and X Ouyang, *J. Phys. Conf. Ser.*, **1053** (2018) 012077.
7. L E Dinca, P Dorenbos, J T M de Haas, V R Bom, and C W E Van Eijk, *Nucl. Instrum. Methods Phys. Res. A*, **486** (2002) 141.
8. P Yang, Ch D Harmon, F P Doty, and J A Ohlhausen, *IEEE Trans. Nucl. Sci.*, **61** (2014) 1024.
9. N Markovic´, Z Siketic´, D Cosic, H K Jung, N H Lee, W T Han, and M Jakšic´, *Nucl. Instrum. Methods Phys. Res. B*, **343** (2015) 167.
10. S Calusi, E Colombo, L Giuntini, A Lo Giudice, C Manfredotti, M Massi, G Pratesi, and E Vittone, *Nucl. Instrum. Methods Phys. Res. B*, **266** (2008) 2306.
11. L Pichon, T Calligaro, V Gonzalez, Q Lemasson, B Moignard, and C Pacheco, *Nucl. Instrum. Methods Phys. Res. B*, **348** (2015) 68.
12. P D Townsend, *Nucl. Instrum. Methods Phys. Res. B*, **286** (2012) 35.
13. P D Townsend, M Khanlary, and D E Hole, *Surf. Coat. Tech.*, **201** (2007) 8160.
14. T Nikbakht, O Kakuee, and M Lamehi-Rachti, *J. Lumin.*, **181** (2017) 246.
15. T Nikbakht, O Kakuee, and M Lamehi-Rachti, *J. Lumin.*, **171** (2016) 154.
16. M Rodríguez-Ramos, M C Jiménez-Ramos, M García-Muñoz, and J García López, *Nucl. Instrum. Methods Phys. Res. B*, **403** (2017) 7.
17. W Kada, T Satoh, S Yamada, M Koka, N Yamada, K Miura, O Hanaizumi, *Nucl. Instrum. Methods Phys. Res. B*, **477** (2020) 66.
18. W Kada, I Sudić, N Skukan, Sh Kawabata, T Satoh, J Susaki, S Yamada, T Sekine, R K Parajuli, M Sakai, K Miura, M Koka, N Yamada, T Kamiya, M Jakšić, and O Hanaizumi, *Nucl. Instrum. Methods Phys. Res. B*, **450** (2019) 157.
19. S Carturan, A Quaranta, A Vomiero, M Bonafini, G Maggioni, and G Della Mea, *IEEE Trans. Nucl. Sci.*, **52** (2005) 748.
20. A Quaranta, Nucl. *Instrum. Methods Phys. Res. B*, **240** (2005) 117.
21. A Quaranta, F Gramegna, V Kravchuk, and C Scian, *Nucl. Instrum. Methods Phys. Res. B*, **266** (2008) 2723.
22. A Quaranta, S Carturan, T Marchi, A Antonaci, C Scian, V L Kravchuk, M Degerlier, F Gramegna, and G Maggioni, *Nucl. Instrum. Methods Phys. Res. B*, **268** (2010) 3155.
23. T Nikbakht, and Y Vosoughi, *Nucl. Instrum. Methods Phys. Res. B*, **537** (2023) 95.
24. M Askari, A Taheri, M Mojtahedzadeh Larijani, A Movafeghi, and H Faripour, *Nucl. Instrum. Methods A*, **941** (2019) 162329.
25. A L Giudice, A Re, D Angelici, S Calusi, N Gelli, L Giuntini, M Massi, and G Pratesi, *Anal. Bioanal. Chem.*, **404** (2012) 277.
26. T Calligaro, Y Coquinot, L Pichon, and B Moignard, *Nucl. Instrum. Methods B*, **269** (2011) 2364.
27. T Calligaro, Y Coquinot, L Pichon, G Pierrat-Bonnefois, P de Campos, A Re, and D Angelici, *Nucl. Instrum. Methods B*, **318** (2014) 139.
28. T Nikbakht, B Yadollahzadeh, and M Zahmatkesh Isfahani, *Nucl. Instrum. Methods B*, **489** (2021) 7.
29. www.SRIM.com
30. J Ch Hsu, and Y Sh Ma, *Coatings*, **9** (2019) 751.